Semiconductor-To-Metal Transitions in Transition-Metal Compounds*

DAVID ADLER†
Division of Engineering and Applied Physics, Harvard University, Cambridge, Massachusetts
and
Center for Materials Science and Engineering, Massachusetts Institute of Technology, Cambridge, Massachusetts

AND

JULIUS FEINLEIB‡
Division of Engineering and Applied Physics, Harvard University, Cambridge, Massachusetts
and
Lincoln Laboratory, Massachusetts Institute of Technology, Lexington, Massachusetts

AND

HARVEY BROOKS AND WILLIAM PAUL
Division of Engineering and Applied Physics, Harvard University, Cambridge, Massachusetts

(Received 20 September 1966)

The theory presented in a previous paper is applied to the transition-metal compounds which are known to exhibit semiconductor-to-metal transitions. In particular, the predictions of the theory are compared with the experimental results of Feinleib and Paul on V_2O_3. Very good agreement is obtained for the magnitude of the energy gap and for its pressure and stress coefficients. The theory appears to be consistent with the available data on the other oxides of vanadium and titanium as well. Band models for all of these compounds are suggested. The effects of spin-disorder scattering and broadening, polaron formation, and nonstoichiometry are considered quantitatively.

I. INTRODUCTION

IN a previous paper,[1] hereafter referred to as I, a theoretical description of semiconductor-to-metal transitions was presented, and several results were obtained which were amenable to experimental testing. In the preceding paper,[2] hereafter referred to as II, the results of new measurements on V_2O_3, which exhibits one of the most striking of such transitions, were given. These measurements offer a direct test of the theory of I. In this paper, we shall compare the theoretical predictions with the experimental results, particularly for the magnitude of the energy gap and its pressure and stress coefficients. We shall also use the theory of I to account for the available data on the other materials which undergo these transitions.

II. COMPARISON OF THEORY WITH EXPERIMENTAL RESULTS

The dependence on temperature of the electrical conductivity of the oxides of vanadium and titanium is given in Fig. 1, which shows the results of the experiments of Morin.[3] All of these oxides except TiO are semiconducting at low temperatures, but undergo transitions to a metallic state at a temperature which we call T_0. In this section, we shall discuss the data on each of these materials in detail.

A. V_2O_3

At room temperature, V_2O_3 has the corundum structure, with rhombohedral symmetry. Near 150°K, a phase transformation occurs; at lower temperature, V_2O_3 has monoclinic symmetry.[4] The monoclinic distortion can be thought of as a shifting of pairs of cations in the corundum basal plane towards one another, resulting

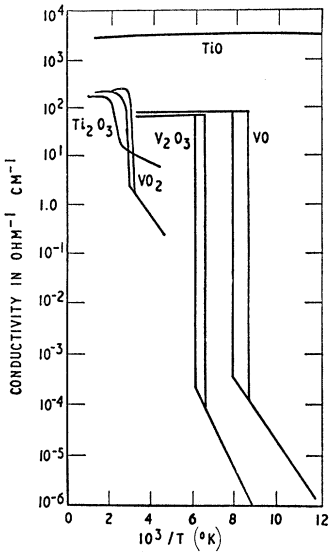

FIG. 1. Conductivity of the lower oxides of titanium and vanadium as a function of temperature (after Morin).

* Research supported by the Advanced Research Projects Agency, by the Office of Naval Research, and by the U. S. Air Force.

† Present address: Center for Materials Science and Engineering, Massachusetts Institute of Technology, Cambridge, Massachusetts.

‡ Present address: Lincoln Laboratory, Massachusetts Institute of Technology, Lexington, Massachusetts.

[1] D. Adler and H. Brooks, second preceding paper, Phys. Rev. **155**, 826 (1967).

[2] J. Feinleib and W. Paul, first preceding paper, Phys. Rev. **155**, 841 (1967).

[3] F. J. Morin, Phys. Rev. Letters **3**, 34 (1959).

[4] E. P. Warekois, J. Appl. Phys. Suppl. **31**, 346S (1960).

in an effective tilting of the c axis. The distortion parameter defined in I is $\epsilon=0.011$. There is also a sharp contraction in volume as V_2O_3 is heated through the transition temperature; recent measurements[5] have shown that this contraction is 3.5%.

The magnetic properties of V_2O_3 have been studied extensively by several techniques, but the results have thus far been inconclusive. Discontinuities have been observed in the magnetic susceptibility near 150°K,[6] and also at an apparent high-temperature transition point near 550°K.[7] However, the temperature dependence of the susceptibility was not that usually associated with an antiferromagnet. Neutron-diffraction experiments have placed an upper limit on the antiferromagnetic moment of 0.2 Bohr magnetons per cation, and were unable to establish any long-range order.[8,9] Nuclear-magnetic-resonance measurements are consistent with antiferromagnetic ordering below 150°K, since the resonance suddenly disappears as the temperature is lowered through the transition point.[10] Most recently, Mössbauer data on 1% Fe in V_2O_3 indicated magnetic ordering at low temperatures, the internal field at the Fe nuclei abruptly vanishing in the metallic state.[11] However, the extrapolated Néel temperature was much larger than 150°K, and the authors conclude that antiferromagnetism cannot entirely account for the semiconductor-to-metal transition.

Paper II reports the results of transport measurements on single crystals of V_2O_3, found to be within 0.3% of stoichiometry. On cooling, a jump in resistivity of a factor of 10^7 was found at $T_0=140$°K. A hysteresis of about 12°K was found on heating. Above the transition temperature, the resistivity increased linearly with temperature and was metal-like. Below T_0, the resistivity increased exponentially with $1/T$, the activation energy varying from 0.12 to 0.18 eV, depending on the sample. These results are in substantial agreement with those of previous workers.[12] The optical measurements at 77°K in II give a direct measurement of the energy gap, which was approximately 0.1 eV. Since, from I, the gap at $T=T_0/2$ is effectively the same as that at $T=0$, we take this value as E_{g0} for V_2O_3. Thus,

$$E_{g0}/kT_0=8.3. \tag{2.1}$$

For V_2O_3, we expect the narrow-band analysis of Sec. III A of I to be appropriate, and thus E_{g0}/kT_0 should be given by Fig. 3. We can then use the experimental result (2.1) to evaluate β:

$$\beta=3.1\,E_{g0}/N. \tag{2.2}$$

This is almost precisely the value obtained in Sec. II D of I for a crystalline distortion ϵ of the order of that in V_2O_3. The study of the transition carried out in II shows that the transition is first order. It is sharp, has a measurable latent heat, and exhibits a hysteresis.

Given that the $T=0$ state of V_2O_3 is that of a narrow-band semiconductor whose gap of 0.1 eV arises from a 1% monoclinic distortion from rhombohedral symmetry, the theory of I predicts a first-order semiconductor-to-metal transition at $T_0=143$°K. At this temperature, there should also be a phase transformation to the rhombohedral structure. All this is in accordance with experiment.

But also, the theory makes a prediction about the pressure and stress coefficients of the energy gap and transition temperature, Eq. (3.17) of I:

$$d\ln T_0/dX=d\ln E_{g0}/dX, \tag{2.3}$$

which can be checked by the results of II. In II, it was found that the transition temperature varied with pressure as

$$d\ln T_0/dP=-2.6\times10^{-5}\ \text{bar}^{-1}, \tag{2.4}$$

where P is the hydrostatic pressure. With uniaxial stress applied parallel to the corundum structure's b axis, the relation between transition temperature and stress was determined to be

$$d\ln T_0/dS=-2.8\times10^{-5}\ \text{bar}^{-1}, \tag{2.5}$$

where S is the stress. With stress applied along the c axis, the uniaxial stress coefficient was at least an order of magnitude smaller:

$$|d\ln T_0/dS|<0.3\times10^{-5}\ \text{bar}^{-1}. \tag{2.6}$$

The pressure and uniaxial stress coefficients for the energy gap were determined from the stress dependence of the activation energy for electrical conductivity. These results can be expressed, in the case of hydrostatic pressure, as

$$d\ln E_{g0}/dP=-2.2\times10^{-5}\ \text{bar}^{-1}, \tag{2.7}$$

whereas with uniaxial stress along the b axis

$$d\ln E_{g0}/dS=-3.0\times10^{-5}\ \text{bar}^{-1}. \tag{2.8}$$

In Sec. IV, we show that the pressure coefficient of contributions to the activation energy from polaron effects and nonstoichiometry is of the order of 10^{-6} bar^{-1}, and thus these contributions do not significantly alter the numbers in (2.7) and (2.8).

A comparison of (2.7) with (2.4) and (2.8) with (2.5) shows that Eq. (2.3) is indeed satisfied within experimental error. Thus, the two major predictions of the theory given in I, (2.2) and (2.3), are verified by the results of II. There is no *a priori* reason for the

[5] S. Minomura and H. Nagasaki, J. Phys. Soc. Japan **19**, 131 (1964).
[6] P. H. Carr and S. Foner, J. Appl. Phys. Suppl. **31**, 344S (1960).
[7] M. Foëx and J. Wucher, Compt. Rend. **241**, 184 (1955).
[8] A. Paoletti and S. J. Pickart, J. Chem. Phys. **32**, 308 (1960).
[9] S. C. Abrahams (private communication).
[10] E. D. Jones, Phys. Rev. **137**, A978 (1965).
[11] T. Shinjo, K. Kosuge, S. Kachi, H. Takaki, M. Shiga, and Y. Nakamura, J. Phys. Soc. Japan **21**, 193 (1966); T. Shinjo, K. Kosuge, M. Shiga, Y. Nakamura, S. Kachi, and H. Takaki, Phys. Letters **19**, 91 (1965).
[12] I. G. Austin, Phil. Mag. **7**,96 1 (1962); A. J. MacMillan, Laboratory for Insulation Research, MIT Technical Report No. 172, 1962 (unpublished); G. Goodman, Phys. Rev. Letters **9**, 305 (1962); M. Foex, Compt. Rend. **223**, 1126 (1946); **227**, 193 (1948); F. J. Morin, Phys. Rev. Letters **3**, 34 (1959).

validity of (2.2) and (2.3), and no other model heretofore suggested predicts these relations. Therefore, the agreement with experiment must be considered as good evidence for the applicability of a model along the lines of I.

The theoretical interpretation of the observed conductivity jump is more subtle. The theory of I predicts that the carrier concentration will jump by a factor of 50 at T_0. The actual jump in conductivity measured in II was a factor of 10^7. This must mean that at T_0 the mobility jumped by roughly 10^5. Furthermore, the activation energy measured in II was between 0.12 and 0.18 eV. The contribution to this from free carriers is just half the energy gap, or 0.05 eV. Thus, the mobility must itself be thermally activated, with activation energy between 0.07 and 0.13 eV in the semiconducting regime. Therefore, we should expect a jump in mobility at the transition of a maximum of $\exp[(0.13\text{ eV})/kT_0]=0.6\times10^5$, which is approximately the observed change. The mobility discontinuity and activation energy are therefore consistent. The origin of this activation of the mobility could be either the large correlation energy expected in such a low electronic density material as V_2O_3, or the energy needed to overcome the Landau trapping of electrons or polarons, if the electron-phonon coupling is large. Below T_0, fewer than 2% of the electrons are free, and the resultant screening is not large enough to reduce the correlation energy and prevent localization. However, at the transition, the sudden increase in carrier concentration by a factor of 50 produces sufficient screening to obtain a true metallic state above T_0. As was pointed out in II, the mean free path and bandwidth in the metallic state of V_2O_3 are about the minimum necessary to give metallic behavior, and V_2O_3 is just a borderline metal above the transition. All this is consistent with the model of V_2O_3 as a very narrow-band material.

As was pointed out in I, the distortion arises because the decrease in electronic energy is linear in the distortion parameter ϵ, whereas the increase in strain energy is quadratic in ϵ. Under pressure, the electronic energy will not change greatly, although the size of the first Brillouin zone will increase and the bands will become wider due to increased overlap, thus reducing the decrease in energy with ϵ. However, for a given distortion, the strain energy will increase and thus the distortion which minimizes the energy will be considerably reduced. This, of course, leads to a smaller energy gap, and, from (2.3), a lower transition temperature. This prediction is borne out by the pressure data, given in (2.4) and (2.7). Furthermore, the distortion which doubles the number of cations in each unit cell is entirely in the basal plane of the corundum structure. Therefore, the variations of E_{g0} and T_0 with uniaxial stress applied along the c axis should not be very large, as is confirmed by the result (2.6). On the other hand, the effect of stress applied along the a axis or b axis should result in a striking decrease in E_{g0} and T_0, as is found in (2.5) and (2.8).

The high-temperature anomaly was also investigated in II, where measurements of resistivity versus temperature from 300 to 800°K were carried out. It was found that the resistivity increases linearly with temperature with the same slope both below and above the high-temperature transition. However, in the vicinity of 550°K, the resistivity undergoes a rather sharp increase over a narrow temperature range. In the region $T_0<T<500$°K, the measured resistivity can be expressed as

$$\rho_L(T)=4.3\times10^{-4}(0.51+0.49T/T_0)\Omega\text{ cm}. \quad (2.9)$$

If we write for the total resistivity up to 800°K

$$\rho(T)\equiv\rho_L(T)+\rho_A(T),$$

where $\rho_L(T)$ is an extrapolation of (2.9), and $\rho_A(T)$ is the anomalous resistivity, then $\rho_A(T)$ is a function which is zero up to 500°K, then sharply rises to a value of 12×10^{-4} Ω-cm by 600°K, above which temperature it remains constant. Such behavior for $\rho_A(T)$ bears a striking resemblance to the spin-disorder resistivity calculated by DeGennes and Friedel,[13] and therefore suggests a magnetic-ordering temperature of 600°K. Wucher[14] and Teranishi and Tarama[15] have concluded from their magnetic-susceptibility data that this is the Néel temperature of V_2O_3. We shall return to this point later.

B. VO

The experimental results for VO are quite similar to those for V_2O_3. VO has rock-salt structure down to 126°K, where there is a crystalline-structure distortion to orthorhombic symmetry. The low-temperature crystal structure has not as yet been reported. Little is known, either, about the magnetic properties of VO, since neutron-diffraction and magnetic-susceptibility measurements have not been performed.

We know a little more about the electrical properties. Morin[3] (see Fig. 1) found that there is a sharp semiconductor-to-metal transition at $T_0=126$°K. The jump in conductivity at T_0 was measured to be a factor of 10^6. Below T_0, the activation energy was $E_A=0.14$ eV. Above T_0, the resistivity increases linearly with T. It can be seen from Fig. 1 that the electrical properties of VO closely resemble those of V_2O_3.

Austin[16] has performed pressure experiments on VO, and has observed the effects of quasihydrostatic pressure on the electrical properties of single crystals of variable composition. From measurements of resistivity as a function of pressure at 94°K, Austin obtained

$$dE_g/dP=-2.9\times10^{-6}\text{ eV bar}^{-1}. \quad (2.10)$$

[13] P. G. De Gennes and J. Friedel, J. Phys. Chem. Solids **4**, 71 (1958).
[14] J. Wucher, Compt. Rend. **241**, 288 (1955).
[15] S. Teranishi and K. Tarama, J. Chem. Phys. **27**, 1217 (1957).
[16] I. G. Austin, Phil. Mag. **7**, 961 (1962).

Since no direct measurement of the energy gap of VO has been made, we can do no better than to assume that the gap is about equal to that of V_2O_3. Using $E_{g0}\sim 0.1$ eV, we find from (3.18) of I

$$E_{g0}/kT_0\sim 9. \tag{2.11}$$

We can now use Austin's results for dT_0/dP to check the approximate validity of (2.3). This relationship provides an important test of the theory. From (2.10), we can express Austin's measurements on the pressure variation of the energy gap as

$$d\ln E_{g0}/dP\approx -29\times 10^{-5}\ \text{bar}^{-1}. \tag{2.12}$$

As mentioned earlier, we shall show in Sec. IV that the pressure coefficients of contributions to E_A from polaron effects and nonstoichiometry are of the order of 10^{-6} bar^{-1}, so that (2.12) probably does represent the variation of the energy gap only.

At 94°K, Austin found

$$d\ln T_0/dP=-32\times 10^{-6}\ \text{bar}^{-1}. \tag{2.13}$$

Comparison of (2.13) with (2.12) demonstrates that (2.3) is roughly satisfied.

We conclude that it is likely that the energy gap in VO arises from a crystalline-structure distortion and has a value of about 0.10 eV, approximately the same as that of V_2O_3. The lower transition temperature of VO seems to be due to a greater change in volume at T_0. This is reflected in a larger value for β in Eq. (2.1) of I, which is also consistent with (2.13) of I. Aside from the slightly lower transition temperature, the characteristics of VO and V_2O_3 seem to be very similar.

C. VO_2

The crystal structure of VO_2 is well known. Above $T=340$°K, the structure is that of rutile, the cations occupying the positions of a body-centered tetragonal lattice. Below 340°K, the symmetry is monoclinic, the structure being that of MoO_2. The low-temperature phase is a distorted rutile structure—the cations which in the rutile phase are collinear and separated by 2.87 Å are slightly noncollinear and spaced alternately 2.65 and 3.12 Å apart.[17] This is a good example of the model of Sec. II D of I—the unit cell is doubled by a distortion of the lattice in one dimension, alternate cations pairing. The parameter ϵ, defined in Sec. II D of I, is 0.04. There is no measurable total volume change at the transition point.[5]

Magnetic measurements on VO_2 have all failed to show any evidence for antiferromagnetism.[18]

The electrical conductivity behavior of VO_2 was studied by Morin[3] (see Fig. 1), who found a sharp semiconductor-to-metal transition at

$$T_0=340\text{°K}, \tag{2.14}$$

the temperature at which the phase transformation takes place. Below T_0, the activation energy was 0.13 eV. The jump in conductivity at T_0 was a factor of 10^2. Recent experiments[19] yield the same value for T_0, but show a discontinuity in σ at T_0 of 3×10^4.

The energy gap has not as yet been measured. Because the narrow-band limit appears to have given good results in the cases of V_2O_3 and VO, we expect it should be at least as appropriate for VO_2, for the cations are V^{4+}, which are smaller in spatial extent than are V^{3+} and V^{2+}. We may also guess that the higher transition temperature of VO_2 is caused by a larger E_{g0}, and this is consistent with the much larger ($\times 4$) value of the distortion parameter ϵ. In I, we found that, using a delta-function potential, the larger the initial gap, the larger the value obtained for β. The most reasonable conclusion is that the final E_{g0}/kT_0 ratio for VO_2 is probably somewhat larger than it is for V_2O_3. As a rough estimate, we shall take

$$E_{g0}\sim 10kT_0 \sim 0.3\ \text{eV}.$$

Pressure measurements on VO_2 have been carried out by Minomura and Nagasaki[5] and by Neuman *et al.*[20] Minomura and Nagasaki measured the variation of T_0 with pressure and found

$$d\ln T_0/dP=-1.4\times 10^{-6}\ \text{bar}^{-1}. \tag{2.15}$$

This is a very small value and contrasts strikingly with the pressure coefficients of V_2O_3 and VO [see (2.4), (2.5), and (2.13)], which are an order of magnitude larger. Neuman *et al.* could not find a shift of T_0 with pressure up to 6 kbar within the 0.5°K scatter in T_0 itself. Thus, they find a still smaller value for $d\ln T_0/dP$ than is given in (2.15).

Neuman *et al.* also measured the change in activation energy with pressure. Their experiments show

$$dE_A/dP=-5.0\times 10^{-7}\ \text{eV bar}^{-1}. \tag{2.16}$$

From their measured value of $E_A=0.44$ eV, (2.16) yields

$$d\ln E_A/dP=-1.1\times 10^{-6}\ \text{bar}^{-1}. \tag{2.17}$$

This is also an order of magnitude smaller than the values for V_2O_3 and VO, given in Eqs. (2.7), (2.8), and (2.12). However, in this case we cannot use (2.17) to evaluate $d\ln E_{g0}/dP$ in order to compare with (2.15) and check the validity of (2.3). For, as we mentioned previously, we show in Sec. IV that the pressure coefficient of the contribution to E_A from polaron effects is of the order of 10^{-7} eV/bar. But, in the case

[17] R. Heckingbottom and J. W. Linnett, Nature **194**, 678 (1962).
[18] J. Umeda, H. Kusumoto, K. Narita, and E. Yamada, J. Chem. Phys. **42**, 1458 (1965); W. G. Rudorff, G. Walter, and J. Stadler, Z. Anorg. Allgem. Chem. **297**, 1 (1958); T. Kawakubo and T. Nakagawa, J. Phys. Soc. Japan **19**, 517 (1964).
[19] R. F. Bongers, Solid State Commun. **3**, 275 (1965); H. Sasaki and A. Watanabe, J. Phys. Soc. Japan **19**, 1748 (1964); I. Kitahiro, A. Watanabe, and H. Sasaki, *ibid.* **21**, 196 (1966).
[20] C. H. Neuman, A. W. Lawson, and R. F. Brown, J. Chem. Phys. **41**, 1591 (1964).

of VO_2, this is just the order of magnitude of dE_A/dP measured in (2.16). Therefore, we cannot calculate $d\ln E_{g0}/dP$, and we can only note that (2.15) and (2.17) are about the same, which has some significance.

The transition in VO_2 appears to be due to a crystalline distortion with little accompanying volume change. Thus, it might be more informative to study the change in conductivity with uniaxial stress than hydrostatic pressure. If our analysis is correct, we should expect the variation in E_{g0} and T_0 with stress applied along the c axis to be significantly larger than the value in (2.15).

D. Ti_2O_3

The structure of Ti_2O_3 is that of corundum at all temperatures down to 4°K.[21] The only region showing any anomaly is the range 450–650°K, where the thermal-expansion parameters sharply increase.

The magnetic structure of Ti_2O_3 is known unambiguously. Abrahams[21] performed neutron-diffraction experiments over the temperature range 1.4 to 711°K and found that antiferromagnetism was present up to a Néel temperature in the vicinity of 660°K. The magnetic structure was monoclinic, strikingly resembling the low-temperature crystal structure of V_2O_3. Abrahams determined that the c-axis pairs were antiferromagnetically aligned, whereas the basal-plane spins were all parallel. The spins were perpendicular to the c axis, thus reducing the symmetry to monoclinic. The magnitude of the antiferromagnetic moment was about 0.2 Bohr magnetons per cation.

Electrical conductivity experiments on Ti_2O_3 have been carried out by Morin[3] (see Fig. 1), who found a semiconductor-to-metal transition at $T_0=450$°K, with a jump in conductivity of a factor of 10. The activation energy determined was very small, $E_A=0.04$ eV. Yahia and Frederikse[22] also demonstrated that a semiconductor-to-metal transition occurs in the vicinity of 450°K, the jump in conductivity being approximately 40, and the activation energy in the semiconducting regime varying from 0.03–0.04 eV. Yahia and Frederikse were also able to measure the Hall effect in Ti_2O_3. From this, they deduced that at low temperatures the concentration of carriers is thermally excited, with an activation energy of 0.03 eV. This is a measure of the band gap, if their material was stoichiometric, as it appeared to be. From this Hall activation energy, we can conclude that $E_{g0}=0.06$ eV.

Abrahams[21] also measured the electrical conductivity of the Ti_2O_3 crystal used for the neutron-diffraction measurements, and found a jump in conductivity of a factor of 40 at about 660°K, instead of 450°K. Thus, T_0 is ill defined at present. However, it is significant that the temperature of the conductivity discontinuity is the same as the Néel temperature.

Since there is no crystalline distortion, the antiferromagnetism alone causes the energy gap, and the theory of Sec. II C of I is applicable. It appears that the effective-mass approximation is more appropriate than the narrow-band limit, for the following reasons. First, we expect the bands to be wider in Ti_2O_3 than in V_2O_3, since the overlap between Ti^{3+} ions should be significantly greater than that between the smaller V^{3+} ions, due to the lower atomic number of Ti. Furthermore, the c-axis pairs are 3% closer in Ti_2O_3, which would tend to increase the overlap, and hence, the bandwidth in the t_0 band, which we shall show in Sec. III, is the band of interest in Ti_2O_3. Second, the presence of antiferromagnetism with such a small moment as 0.2 μ_B per cation is an indication of bandwidth larger than the exchange splitting.[23] Third, the small (less than 0.01 eV) contribution to the activation energy for conduction from effects other than the band gap is evidence for smaller polaron effects in Ti_2O_3 than in V_2O_3, and so of wider bands. Fourth, from the discussion of I, a lack of crystalline distortion is a wide-band characteristic.

The presence of an extra parameter m^* affords a greater degree of freedom in the calculation of the transition temperature in this case than in the narrow-band limit. However, Yahia and Frederikse[22] were able to calculate the effective mass of holes in Ti_2O_3 from their Hall and thermoelectric data, and they found $m_h=5m$. This is still another argument favoring the use of the effective-mass approximation. From the small magnitude of the gap, it is clear that Boltzmann statistics are inappropriate, and the general expression (3.23) of I must be studied. A careful calculation[23] shows

$$E_{g0}/kT_0=1.2. \tag{2.18}$$

Although the effective-mass approximation will not be valid over the whole range of occupied states, this result is probably still correct in order of magnitude, since the general shape of the bands given by Eq. (3.21) of I is still similar. Equation (2.18) predicts $T_0=580$°K, which is within the experimental range. This solution turns out to be a second-order, rather than first-order, transition, which also appears to agree with the experimental situation. No hysteresis is thus predicted, and none occurs. Also, for this solution, the jump in carrier concentration at the transition is much smaller than for the oxides of vanadium. More important, the much wider bands of Ti_2O_3 should produce sufficient screening so that the mobility in the semiconducting state is not thermally activated. Evidence of this has already been noted, there being only very small nongap contributions to the activation energy. These points should be reflected in larger conductivity in the semiconducting region and a smaller jump in conductivity at the transition. As can be seen in Fig. 1, this is indeed the observed situation.

[21] S. C. Abrahams, Phys. Rev. **130**, 2230 (1963).
[22] J. Yahia and H. P. R. Frederikse, Phys. Rev. **123**, 1257 (1961).
[23] D. Adler (to be published).

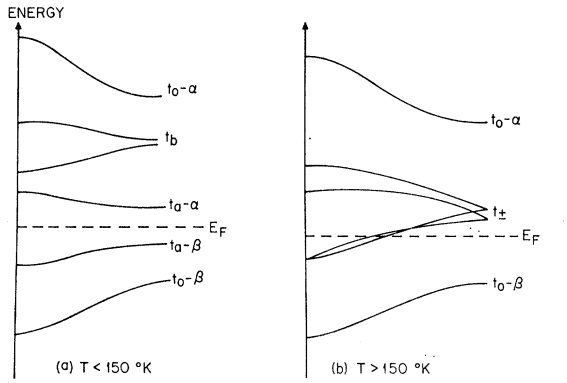

FIG. 2. Suggested band scheme for V_2O_3.

III. MODELS FOR BAND STRUCTURE

In this section, we shall try to piece together the approximate band structure of these oxides. Since some critical information is missing about every one of these materials, the band models presented here are speculative, but they are all consistent with both the symmetry and the electrical properties of the crystals.

A. V_2O_3

For the corundum phase of V_2O_3, the trigonal field will split the t_{2g} band into a t_0 and a $t_\pm$ band. The t_0 band is associated with orbitals directed along the c axis, the $t_\pm$ band with orbitals primarily in the basal plane. Below 150°K, the crystal has monoclinic symmetry, and the $t_\pm$ band is split into two sub-bands, which we shall call the t_a band and the t_b band. The c-axis pairs have the closest cation-cation distances, and these cations are in octahedral arrays of anions which share a common face. We should therefore expect a relatively large bonding-antibonding splitting of the t_0 band. The monoclinic distortion, as we have demonstrated in Sec. II, leads to the pairing of cations in the basal plane, albeit with a somewhat larger cation-cation distance than along the c axis. Thus, the bonding-antibonding splitting of the t_a and t_b bands is relatively small. We infer that the t_0 bonding band is lowest for V_2O_3, and that it is separated from the t_0 antibonding band by an energy E_{g2}. The t_a bonding band is next lowest, and it is separated from the t_a antibonding band by an energy E_{g1}. We assume the situation is as given in Fig. 2(a). Since the narrow-band limit appeared to give good results for V_2O_3, we have drawn the bands as quite narrow, and thus there is no overlap. We shall give an order-of-magnitude estimate of the bandwidth below. Each of the six sub-bands contains one state per cation. Thus, for V_2O_3, with two $3d$ electrons per V^{3+} ion, the bottom two bands are exactly filled at $T=0$, while the top four bands are completely empty. The material is thus a narrow-band semiconductor with an energy gap E_{g1}. We determined in Sec. II that $E_{g1}=0.10$ eV. The theory presented there shows that at $T_0=150$°K, a phase transformation occurs due to the breaking up of the basal-plane pairs, changing the crystal structure to the higher-symmetry rhombohedral phase.

Above 150°K, the situation is now as shown in Fig. 2(b). In this temperature range, V_2O_3 is a metal, the $t_\pm$ band being $\frac{1}{4}$ filled. Thus T_0 is also the temperature at which a semiconductor-to-metal transition occurs, as is experimentally observed.

But we recall that there was another anomaly in the electric and magnetic properties in V_2O_3, at $T_t\sim600$°K, and that the resistivity in this region showed the characteristics of a spin-disorder scattering [see the discussion following Eq. (2.9)]. If V_2O_3 is antiferromagnetic at $T=0$, then antiferromagnetism would contribute to the t_0 band splitting. In particular, the antiparallel spin arrangement of c-axis pairs is just the magnetic configuration found by Abrahams[21] in Ti_2O_3. We would expect the same spin configuration in V_2O_3 as in the structurally similar Ti_2O_3, so this is a reasonable hypothesis. Furthermore, antiferromagnetic-paramagnetic transitions are of second order, as the high-temperature V_2O_3 transition appears to be experimentally. We shall find, in Sec. IV, that the spin-disorder resistivity deduced from Sec. II is consistent with the exchange energy estimated from taking T_t as the Néel temperature of V_2O_3. Since the antiferromagnetic moment in V_2O_3, if it exists at all, must be very small, it follows that the width of the two bands must be large compared with exchange splitting E_{g2}.

B. Ti_2O_3

In Ti_2O_3, the trigonal field splits the t_{2g} band into t_0 and $t_\pm$ sub-bands. Experimentally as well as theoretically, the t_0 band turns out to have lower energy than the $t_\pm$ band.[24] Since the structure of Ti_2O_3 below 600°K is the same as that of V_2O_3 between 150 and 600°K, we might expect similar band schemes in these temperature ranges. However, as we indicated in Sec.

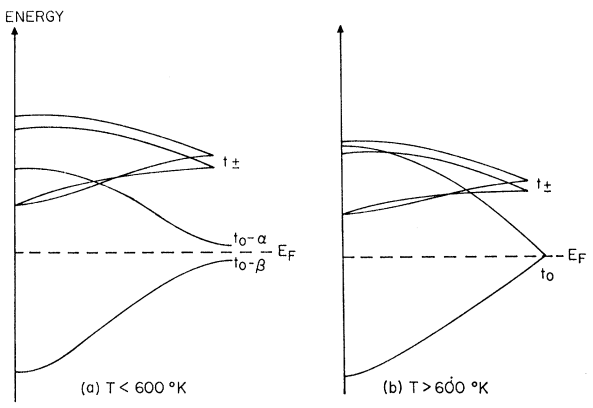

FIG. 3. Suggested band scheme for Ti_2O_3.

[24] M. Blume (to be published).

II, the bands in Ti_2O_3 are much wider than those in V_2O_3.

The band scheme for Ti_2O_3 below T_0 is given in Fig. 3(a). Since there is only one $3d$ electron present per cation, the t_0 band, which corresponds to electrons primarily with spins on their own sublattice (analogous to the bonding bands in V_2O_3), is exactly filled, while all higher t_{2g} bands are completely empty. In this temperature range, Ti_2O_3 is therefore a semiconductor, with a gap of $E_g=0.06$ eV, brought about by c-axis antiferromagnetism. The theory then predicts a semiconductor-to-metal transition at about $T_0=600°K$. Above 600°K, the band situation is given in Fig. 3(b). In this range, the t_{2g} bands are $\frac{1}{6}$ filled, and the material is metallic.

It is, perhaps, surprising that with such a small gap, and such a broad band, Ti_2O_3 is a semiconductor rather than a semimetal below the transition. Much more detailed band-structure calculations would be needed to rigorously establish the model shown in Fig. 3(a) on theoretical grounds.

C. VO and TiO

Below 126°K, VO undergoes a distortion to orthorhombic symmetry, so that the t_{2g} bonding and antibonding bands are each split into three sub-bands, which we call t_x, t_y, t_z. The exact low-temperature structure is as yet unknown, so that we cannot make any statement about the relative positions of these sub-bands. We arbitrarily take the orthorhombic lattice parameters to be smallest along the x axis, largest along the z axis. In the case of VO, we expect the bands to be wider than in V_2O_3, but probably not so wide as in Ti_2O_3, since the V^{2+} ion is smaller in extent than is the Ti^{3+} ion. Whether or not there is overlap between the sub-bands is irrelevant in VO, as long as there is a real gap between the t_x bonding and the t_x antibonding bands. From experiment, we know that this gap exists and is about 0.1 eV. The band structure of VO below 126°K is sketched in Fig. 4(a). There are three $3d$ electrons per cation, and so the lower three sub-bands are just filled, while the upper three sub-bands are completely empty. Thus VO is a semiconductor, whose gap of 0.10 eV is brought about by a crystalline distortion. The theory predicts a transition at $T_0=126°K$ to the situation as shown in Fig. 4(b). Above T_0, VO has a $\frac{1}{2}$ filled t_{2g} band and is metallic.

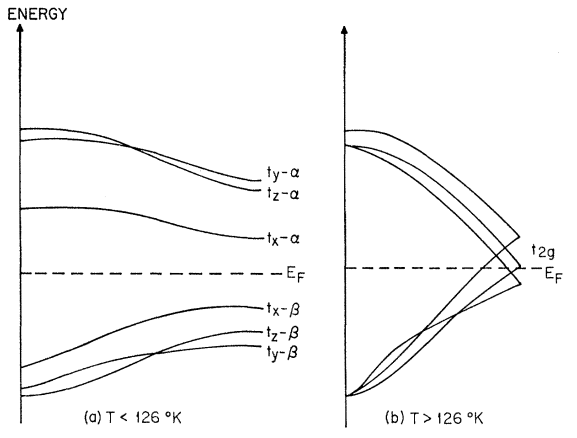

FIG. 4. Possible band scheme for VO.

Note that TiO retains rock-salt structure down to at least 4°K. The presence of antiferromagnetism has not been established, but since TiO contains only two $3d$ electrons per Ti^{2+} ion, it must exhibit metallic behavior at all temperatures. As can be seen from the results of Morin's work[3] (see Fig. 1), this is the case down to at least 1.5°K.

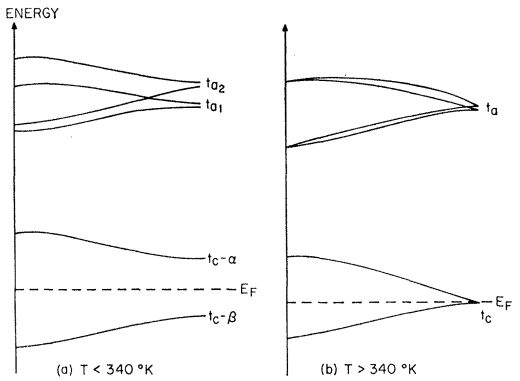

FIG. 5. Possible band scheme for VO_2.

D. VO_2

The rutile phase of VO_2 has tetragonal symmetry, and the t_{2g} band is split into a t_a sub-band with 4 states per cation and a t_c band with 2 states per cation. Since c is considerably smaller than a in rutile VO_2, we expect the t_c band to be well below the t_a band. At low temperatures, the crystal undergoes a distortion to monoclinic symmetry, with the c-axis cations of the rutile structure forming pairs. This monoclinic distortion has two effects. The t_a band is split into sub-bands, which we shall call the t_{a1} and the t_{a2} bands. But, more important, the t_c band is split into bonding and antibonding sub-bands by the pairing along the c axis, which is a classic example of the theory of crystalline distortion given in Sec. II D of I. The distortion parameter ϵ is rather large, which tends to bring about a large energy gap, estimated in Sec. II to be 0.3 eV. The band structure below $T_0=340°K$ is outlined in Fig. 5(a). There is just one $3d$ electron per V^{4+} ion, just filling the t_0-β band, and all higher bands are empty. The theory predicts a transformation at T_0 to the rutile structure. Above 340°K, the band structure is given in Fig. 5(b). It can be seen that the t_c band is $\frac{1}{2}$ filled, resulting in a semiconductor-to-metal transition at 340°K, as is observed.

IV. DISCUSSION

A. The Metallic State of V_2O_3

The measurement of the latent heat of transition in II, taken together with the theory of I, enables us to draw some quantitative conclusions about the metallic state of V_2O_3. In particular, we can calculate the Fermi energy and from this value estimate the metallic bandwidth. From the free-energy expressions of I, with $\delta=\frac{1}{3}$ as is appropriate for V_2O_3, the entropy change per molecule at the transition is

$$\Delta S=S_{\text{met}}-S_{\text{semicond.}}$$
$$=2.34k.$$

This represents the sum of the electronic and lattice distortion contributions, and produces a latent heat at the transition temperature of

$$L=T_0\Delta S=0.030 \text{ eV/molecule}.$$

The actual latent heat found in II was 0.044 eV/molecule. Assuming that the entropy change due to the contraction of the lattice at T_0 is small, we can account for the additional latent heat by introducing finite width bands. The Fermi energy can be estimated by taking an effective Fermi surface which is spherical and assuming parabolic bands. This leads to

$$E_F=\pi^2(kT_0)^2/L_{\text{elec}}=0.10 \text{ eV}.$$

This is a reasonable magnitude for E_F, consistent with the ideas of an extremely narrow band which were used in Secs. II and III. With this value for E_F, the bandwidth in the metallic state can be estimated as $E_b\sim 8kT_0$, so that the approximation of Boltzmann statistics is valid. Using this E_F, we can calculate the effective mass of electrons in the metallic state from

$$E_F=(\hbar^2/2m^*)(3\pi^2N)^{2/3}.$$

This results in an effective mass of 50 times the electronic mass, roughly what we might expect for V_2O_3. This magnitude is also consistent with that estimated from measurements of the plasma frequency,[25] $m^*=45m$.

B. Spin-Disorder Scattering

We shall apply the spin-disorder scattering theory of DeGennes and Friedel[13] in an attempted explanation of the resistivity anomaly in V_2O_3 at high temperatures. There are two main effects of this type of scattering, which was completely ignored in Sec. III of I. First, there is a contribution to the resistivity, which is small when the spins are highly ordered, but adds a term independent of temperature after long-range order disappears. Second, there is a broadening of the bands, which will affect the relations developed between E_{g0} and T_0.

[25] J. Feinleib (unpublished).

Let us assume that V_2O_3 is antiferromagnetic up to the high-order transition temperature, $T_t=600$°K. Estimating the exchange energy from the theory of Secs. II C and III B of I, we find $E_{\text{ex}}\approx 4kT_t=0.2$ eV. The exchange energy is due to the coherent scattering arising from the exchange potential. But it is the incoherent scattering caused by this same potential which gives rise to the spin-disorder resistivity. Using the Born approximation and the extreme simplifications of spherical energy surfaces and quasifree electrons, the spin-disorder resistivity above T_N can easily be estimated from the energy gap.

Under the assumption of quasifree electrons, the energy gap can be expressed as twice the Fourier component of the exchange potential:

$$E_{g0}=2V_{\mathbf{k}\mathbf{k}'}\equiv 2\int d\mathbf{r}\,\Psi_{\mathbf{k}'}^*(\mathbf{r})V_{\text{ex}}(\mathbf{r})\Psi_{\mathbf{k}}(\mathbf{r}),$$

where $\mathbf{k}-\mathbf{k}'$ is twice the Fermi momentum $\mathbf{k}_F$. For the case of V_2O_3, this gives $V_{kk'}=0.1$ eV. For spherical energy surfaces, the resistivity can be expressed[26]

$$\rho_{s0}=\frac{3}{16\pi\hbar e^2v^2N}\int\int d\Omega d\Omega'\,|V_{\mathbf{k}\mathbf{k}'}|^2(1-\cos\theta). \quad (4.1)$$

Performing the integrations, (4.1) can be written

$$\rho_{s0}=\frac{3\pi}{8}\left(4-\frac{\pi^2}{4}\right)\frac{m(V_{\mathbf{k}\mathbf{k}'})^2}{\hbar e^2NE_F}\left(\frac{m^*}{m}\right). \quad (4.2)$$

Using the values $m^*=50m$, $E_F=0.10$ eV estimated above for the high-temperature phase of V_2O_3, Eq. (4.2) yields

$$\rho_{S0}=12\times 10^{-4}\ \Omega\text{ cm}. \quad (4.3)$$

This is just the value of $\rho_A(T)$ measured in II for the anomalous resistivity increase in V_2O_3 above 600°K. Although the values of Fermi energy and of the effective mass used in (4.2) are just rough approximations, they can both be arrived at by two different methods and we thus do not expect too much variation. Therefore, the agreement between theory and experiment can be considered quite good. However, we cannot prove the existence of antiferromagnetism in V_2O_3 by such arguments, since the agreement could be accidental.

It is also important to estimate the amount of broadening of the bands brought about by spin disorder. Using the same assumptions as in Eq. (4.1), the perturbing potential due to spin disorder can be expressed as half the change in energy gap:

$$\langle V_{\text{pert}}\rangle=\tfrac{1}{2}(E_{g0}-E_g). \quad (4.4)$$

Using Eq. (2.18) of I for the change in energy gap, we obtain from (4.4)

$$\langle V_{\text{pert}}\rangle=(n/N)E_{g0}.$$

[26] J. B. Gibson, J. Phys. Chem. Solids **1**, 27 (1956).

Thus, the mean-square deviation in energy due to spin disorder is

$$(\Delta E)^2=E_{g0}^2(n/N)^2. \tag{4.5}$$

Equation (4.5) shows that the effect of spin-disorder broadening is similar to the modification brought about by a Gaussian spread around delta-function bands in the narrow-band limit, except that the spread is no longer constant, but depends on the amount of spin disorder, and thus on n. We have already worked out the case of a Gaussian spread in detail in Sec. III A of I. Using (4.5) as the value for λ^2 in the antiferromagnetic analogue of (3.20) of I, we obtain

$$E_{g0}/kT_0=4.5. \tag{4.6}$$

Thus, spin-disorder broadening lowers the transition temperature about 10%.

C. Polaron Effects

We now consider the possibility of the formation of small polarons in the vanadium oxides. According to Holstein,[27] conduction in a polaron band, which should dominate at sufficiently low temperatures, decreases exponentially with increasing temperature, while conduction which proceeds by uncorrelated polaron hopping between adjacent sites has just the opposite temperature characteristic. The latter behavior is obtained experimentally for the oxides of vanadium in their range of semiconduction. When polaron hopping is dominant, the resultant activation energy is[27]

$$(E_A)_{\rm pol}=\frac{K}{\pi}\int_0^\pi \frac{dk(1-\cos k)}{\omega_k^2}, \tag{4.7}$$

where K is a constant depending on the mass of the ions and the strength of the electron-phonon interaction, and ω_k are the optical-phonon frequencies. Assuming for the optical phonons that $\omega_k=\omega_0$, we obtain from (4.7)

$$(E_A)_{\rm pol}=K/\omega_0^2. \tag{4.8}$$

Although the mean-phonon frequency can be expected to increase somewhat with pressure, it is unlikely that it will change sufficiently to account for the decrease in activation energy by a factor of 2 at pressures of 20 kbars, as measured in II for V_2O_3 and by Austin[16] for V_2O_3 and VO. Thus, it is unlikely that thermally activated hopping of polarons is the major contributor to the conductivity.

We can make a quantitative estimate of the contribution of polaron effects to the pressure coefficient of the total activation energy from (4.8), using the pressure dependence of ω_0 obtained from a Gruneisen relation[28]

$$d\ln\omega_0/d\ln V=-\alpha/\rho K C_v, \tag{4.9}$$

where α is the thermal expansion coefficient, ρ the density, and C_v the specific heat at constant volume. For V_2O_3, $\alpha=40\times10^{-6}(°K)^{-1}$, $\rho=5.0$ g/cm^3, $C_v=6.7\times10^6$ dyn cm/g°K, so that

$$\frac{d\ln(E_A)_{\rm pol}}{dP}=-\frac{2d\ln\omega_0}{dP}=-2.4\times10^{-6}\ \text{bar}^{-1}. \tag{4.10}$$

Comparing (4.10) to (2.7), (2.8), and (2.12), we see that the contribution to the pressure coefficient of the activation energy from polaron effects is smaller by an order of magnitude than the observed value in V_2O_3 and VO. However, from (4.10) and (2.17), the polaron contribution to the activation energy of VO_2 may be quite significant.

It is, perhaps, worth noting that the decreases in resistivity with pressure in NiO, CoO, CuO, and MnO[29] are smaller than in V_2O_3 and VO. For these materials, the calculated changes in ω_0 with pressure using (4.10) can account completely for the experimental pressure coefficients of E_A.

D. Effects of Nonstoichiometry

It is also important to consider the effects of deviations from stoichiometry, particularly in the materials under consideration, which are difficult to obtain in their pure form. For simplicity, we shall consider the case where there is a given number N_d of donor levels per unit volume. The case where acceptor levels are present follows analogously. We shall take the case of a crystalline distortion in a narrow band material, with a view towards applying the results to V_2O_3.

We start with the expression (3.7) of I and take $n=n_i+N_d$ and $p=n_i$. This assumes that all donor levels are shallow. At extremely low temperatures, it is possible to have electrons partly trapped on the donor sites; however, such temperatures are not reached in practice, so we shall ignore this region. At higher temperatures, the donors become completely ionized, and saturated extrinsic conductivity dominates. At still higher temperatures, intrinsic conductivity begins to become important, and if n_i becomes large compared to N_d, intrinsic conductivity could eventually dominate.

If we take $\bar{\delta}=\frac{1}{3}$, the value appropriate to V_2O_3, then substitution in (3.7) and introduction of the strain energy leads by a similar procedure to I to an expression analogous to (3.12) of I:

$$\frac{F(x_i,x_d,y)}{2NkT}=-\frac{y}{6}(1-2x_d-3x_i)^2+\frac{x_d+x_i}{2}\ln(x_d+x_i)$$
$$+\frac{x_i}{2}\ln x_i+\frac{1-x_d-x_i}{2}\ln(1-x_d-x_i)+\frac{1-x_i}{2}\ln(1-x_i), \tag{4.11}$$

[27] T. Holstein, Ann. Phys. (N. Y.) 8, 325 (1959); 8, 343 (1959).
[28] N. F. Mott and H. Jones, *Theory of Metals and Alloys* (Dover Publications, Inc., New York, 1936), p. 19.
[29] S. Minomura and H. G. Drickamer, J. Appl. Phys. 34, 3043 (1963).

where $x_d \equiv N_d/N$, $x_i \equiv n_i/N$, and $y \equiv E_{g0}/2kT$. The metallic free energy, the generalization of (3.16) of I, for $x_d \ll 1$, is

$$F_{\text{Met}}/2NkT = -0.693 + x_d^2. \tag{4.12}$$

Minimization of (4.11) with respect to x_i gives the carrier concentration as a function of temperature:

$$y = \left[\frac{1}{2}\ln\frac{(1-x_i)(1-x_d-x_i)}{x_i(x_d+x_i)}\right] \Big/ (1-2x_d-3x_i). \tag{4.13}$$

In the Boltzmann limit, in which we may take x_i, $x_d \ll 1$, (4.13) can be approximated by

$$x_i = \frac{x_d}{2}\left\{\left[1+\frac{4e^{-2y(1-2x_d-3x_i)}}{x_d^2}\right]^{1/2} - 1\right\}. \tag{4.14}$$

In the extrinsic range, $x_i \ll x_d$, and (4.14) becomes

$$x_i = \frac{e^{-2y(1-2x_d-3x_i)}}{x_d}, \tag{4.15}$$

which has the solution

$$x_i = \frac{e^{-2y(1-2x_d)}}{x_d}\mathfrak{N}[6ye^{-2y(1-2x_d)}/x_d], \tag{4.16}$$

where $\mathfrak{N}(\tau)$ is the function defined in (3.15) of I. From (4.16), we obtain the critical point for a second-order transition as

$$y_c = (x_d/6e)\mathfrak{N}[e^{x_d(1-2x_d)/3e}]. \tag{4.17}$$

This expression is valid only if the value of x_i at y_c from (4.16) is still much smaller than x_d, but for donor concentrations of over 3% this will be the case. Of course, as in the stoichiometric case, the metallic free energy drops below the semiconducting free energy at a temperature lower than (4.17). Thus, a first-order transition will occur at a temperature given by

$$\frac{E_{g0}}{kT_0} = 8.10(1+4x_d) + \frac{x_d}{2}\ln\frac{1}{x_d}. \tag{4.18}$$

Equation (4.18) shows that donor levels decrease the transition temperature somewhat. As an example, a donor concentration of 5% will decrease T_0 by about 9%. Note that the transition temperature is not drastically changed, even though there is virtually no intrinsic conductivity in the semiconducting region. This shows that Eq. (2.3) is still valid when saturated extrinsic conductivity dominates. Note also that (4.17) shows that the second-order transition temperature is actually raised in this region. This is not too surprising since this transition is dependent primarily on the intrinsic conductivity. A physical effect of the raising of the second-order transition point could be manifested in the width of the hysteresis, which should be directly related to the difference between the first- and second-order transition temperatures. Equations (4.17) and (4.18) together thus indicate that a lack of stoichiometry should widen the hysteresis considerably.

When the donor concentration is not this high, intrinsic conductivity becomes important. For concentrations much less than 2%, the critical intrinsic conductivity given in (3.19) of I, we may take $x_i \gg x_d$. To first order in x_d, we then obtain

$$E_{g0}/kT_0 = 8.3(1+1.4x_d). \tag{4.19}$$

Equation (4.19) shows that small donor concentration lowers the transition temperature a very small percentage. In the range where intrinsic conductivity dominates, it can be seen that the second-order transition temperature T_c decreases negligibly as

$$E_{g0}/kT_c = 6.60(1+0.003x_d).$$

In arriving at (4.18) and (4.19) we have neglected terms of second order in x_d. The apparent small discrepancy between (4.19) with $x_d = 0$ and the expression (3.18) of I is due to the fact that the latter is a full Fermi calculation, whereas (4.18) and (4.19) are Boltzmann approximations. It is interesting to note that when $x_d = 3\%$, the lower limit for validity of (4.18), (4.18) is numerically almost identical to (4.19) and has almost the same slope.

Experiments on V_2O_3 samples of varying stoichiometry were carried out by MacMillan,[30] who reduced V_2O_5 in hydrogen at different temperatures. In measurements down to 100°K, it was found that the transition temperature was independent of composition, in accordance with our results (4.18) and (4.19). Activation energy appeared to be constant with temperature in the semiconducting region and varied only slightly with composition, indicating that conduction is primarily intrinsic in this range.

In the wide-band solution of Sec. III B of I, which gave good results for Ti_2O_3, the transition temperature varies much more with impurity content than do the narrow-band solutions (4.18) and (4.19). The result for Ti_2O_3, (2.18), is particularly sensitive to a small donor or acceptor concentration. This is perhaps the explanation for the wide variation in T_0 from sample to sample observed in Ti_2O_3.

[30] A. J. MacMillan, Laboratory for Insulation Research, MIT Technical Report No. 172, 1962 (unpublished).